

Evaluation of terrestrial carbon cycle models for their response to climate variability and to CO₂ trends

SHILONG PIAO*†, STEPHEN SITCH‡, PHILIPPE CIAIS§, PIERRE FRIEDLINGSTEIN‡, PHILIPPE PEYLIN§, XUHUI WANG*, ANDERS AHLSTRÖM¶, ALESSANDRO ANAV‡, JOSEPH G. CANADELL ||, NAN CONG*, CHRIS HUNTINGFORD**, MARTIN JUNG††, SAM LEVIS‡‡, PETER E. LEVY§§, JUNSHENG LI¶¶, XIN LIN¶¶, || ||, MARK R LOMAS***, MENG LU†††, YIQI LUO‡‡‡, YUECUN MA*, RANGA B. MYNENI§§§, BEN POULTER§, ZHENZHONG SUN*, TAO WANG§, NICOLAS VIOVY§, SOENKE ZAEHLE†† and NING ZENG¶¶¶

*Sino-French Institute for Earth System Science, College of Urban and Environmental Sciences, Peking University, Beijing 100871, China, †Institute of Tibetan Plateau Research, Chinese Academy of Sciences, Beijing 100085, China, ‡College of Engineering, Computing and Mathematics, University of Exeter, Exeter EX4 4QF, UK, §Laboratoire des Sciences du Climat et de l'Environnement, CEA CNRS UVSQ, Gif-sur-Yvette 91191, France, ¶Department of Physical Geography and Ecosystem Science, Lund University, Sölvegatan 12, Lund SE 223 62, Sweden, || Global Carbon Project, Commonwealth Scientific and Industrial Research Organization, Marine and Atmospheric Research, Canberra, Australia, **Centre for Ecology and Hydrology, Benson Lane, Wallingford, OX10 8BB, UK, ††Max Planck Institute for Biogeochemistry, P.O. Box 10 01 64, Jena 07701, Germany, ‡‡National Center for Atmospheric Research, Boulder, CO 80301, USA, §§Centre for Ecology and Hydrology, Bush Estate, Penicuik, Midlothian EH26 0QB, UK, ¶¶State Key Laboratory of Environmental Criteria and Risk Assessment, Chinese Research Academy of Environmental Sciences, Beijing 100012, People's Republic of China, || || College of Water Sciences, Beijing Normal University, Beijing 100875, People's Republic of China, ***Department of Animal & Plant Sciences, University of Sheffield, Sheffield S10 2TN, UK, †††Institute of Biodiversity Science, Fudan University, 220 Handan Road, Shanghai 200433, China, ‡‡‡Department of Microbiology and Plant Biology, University of Oklahoma, Norman, OK 73019, USA, §§§Department of Geography and Environment, Boston University, 675 Commonwealth Avenue, Boston, MA 02215, USA, ¶¶¶Department of Atmospheric and Oceanic Science, University of Maryland, College Park, MD 20740, USA

Abstract

The purpose of this study was to evaluate 10 process-based terrestrial biosphere models that were used for the IPCC fifth Assessment Report. The simulated gross primary productivity (GPP) is compared with flux-tower-based estimates by Jung *et al.* [*Journal of Geophysical Research* **116** (2011) G00J07] (JU11). The net primary productivity (NPP) apparent sensitivity to climate variability and atmospheric CO₂ trends is diagnosed from each model output, using statistical functions. The temperature sensitivity is compared against ecosystem field warming experiments results. The CO₂ sensitivity of NPP is compared to the results from four Free-Air CO₂ Enrichment (FACE) experiments. The simulated global net biome productivity (NBP) is compared with the residual land sink (RLS) of the global carbon budget from Friedlingstein *et al.* [*Nature Geoscience* **3** (2010) 811] (FR10). We found that models produce a higher GPP (133 ± 15 Pg C yr⁻¹) than JU11 (118 ± 6 Pg C yr⁻¹). In response to rising atmospheric CO₂ concentration, modeled NPP increases on average by 16% (5–20%) per 100 ppm, a slightly larger apparent sensitivity of NPP to CO₂ than that measured at the FACE experiment locations (13% per 100 ppm). Global NBP differs markedly among individual models, although the mean value of 2.0 ± 0.8 Pg C yr⁻¹ is remarkably close to the mean value of RLS (2.1 ± 1.2 Pg C yr⁻¹). The interannual variability in modeled NBP is significantly correlated with that of RLS for the period 1980–2009. Both model-to-model and interannual variation in model GPP is larger than that in model NBP due to the strong coupling causing a positive correlation between ecosystem respiration and GPP in the model. The average linear regression slope of global NBP vs. temperature across the 10 models is -3.0 ± 1.5 Pg C yr⁻¹ °C⁻¹, within the uncertainty of what derived from RLS (-3.9 ± 1.1 Pg C yr⁻¹ °C⁻¹). However, 9 of 10 models overestimate the regression slope of NBP vs. precipitation, compared with the slope of the observed RLS vs. precipitation. With most models lacking processes that control GPP and NBP in addition to CO₂ and climate, the agreement between modeled and observation-based GPP and NBP can be fortuitous. Carbon–nitrogen interactions (only separable in one model) significantly influence the simulated response of carbon cycle to temperature and atmospheric CO₂ concentration, suggesting that nutrients limitations should be included in the next generation of terrestrial biosphere models.

Keywords: carbon cycle, CO₂ fertilization, model evaluation, precipitation sensitivity, temperature sensitivity

Received 8 February 2013; revised version received 8 February 2013 and accepted 17 February 2013

Correspondence: Shilong Piao, e-mail: slpiao@pku.edu.cn

Introduction

The human perturbation of the carbon cycle largely drives climate change, directly through emissions but also via climate feedbacks on natural carbon sources and sinks. The terrestrial carbon cycle has been modeled to be particularly sensitive to current and future climate and atmospheric CO₂ changes, but regional patterns and mechanisms of terrestrial carbon sources and sinks remain uncertain (Schimel *et al.*, 2001; Houghton, 2007). During the past decades, considerable efforts have been made to develop process-based carbon cycle models, as tools to understand terrestrial carbon mechanisms and fluxes at local, regional, continental, and global scales (Moorcroft, 2006; Huntingford *et al.*, 2011). Models were applied to hindcast historical changes (Cramer *et al.*, 2001; Piao *et al.*, 2009a) and to forecast future changes (Friedlingstein *et al.*, 2006; Sitch *et al.*, 2008). Carbon cycle models have been tested against CO₂ fluxes measured by eddy covariance technique at sites around the world (Sitch *et al.*, 2003; Krinner *et al.*, 2005; Jung *et al.*, 2007; Stöckli *et al.*, 2008; Keenan *et al.*, 2012; W. Wang, P. Ciais, R. Nemani, J. Canadell, S. Piao, S. Sitch, M. White, H. Hashimoto, C. Milesi, R. Myneni, submitted), satellite-based leaf area index (LAI) retrieval products (Lucht *et al.*, 2002; Piao *et al.*, 2006, 2008), and observed vegetation productivity and carbon storage (Randerson *et al.*, 2009). And yet, it is difficult to draw a clear picture of model performance and shortcomings from the current model-benchmarking literature dealing with the global terrestrial carbon cycle. The reasons for this are several: (i) *in situ* high-quality measurements are very sparse and short term, and often cannot be extrapolated readily to larger spatial and temporal scales; (ii) satellite measurements provide only indirect proxies of carbon variables; (iii) atmospheric CO₂ evaluates the combination of a terrestrial carbon model, atmospheric transport model and potentially ocean carbon models, and therefore the results depend on the choice of the atmospheric transport model and its bias (Stephens *et al.*, 2007); (iv) uncertainties associated with measurements are often not reported, which generates type-1 error (a model is estimated to be realistic but the benchmark measurement is not accurate enough to say this) and type-2 error (a model is estimated to be erroneous because the benchmark data were inaccurate or not relevant); and (v) several recent studies have documented prototype benchmark schemes for the carbon cycle (Randerson *et al.*, 2009; Cadule *et al.*, 2010; Blyth *et al.*, 2011), however, a community-wide set of agreed benchmark tests and performance indicators is currently still under development.

Current coupled climate-carbon models used in the fourth and fifth Assessment Reports of the Intergovern-

mental Panel on Climate Change (IPCC) generally project a positive feedback between global warming and the reduction in terrestrial carbon sinks in the 21st century (Denman *et al.*, 2007). In some instances, and for some regions (Tropical forest, regions with frozen vulnerable soil carbon stores) the positive feedbacks become stronger over time surpassing the CO₂-induced fertilization negative feedback, making the land surface to eventually become an overall source (Cox *et al.*, 2000). Characterizing climate and CO₂ feedbacks on the carbon cycle has important implications for mitigation policies designed to stabilize greenhouse gas levels (Matthews, 2005). The magnitude of the feedback varies markedly among models (Friedlingstein *et al.*, 2006). For the SRES-A2 CO₂ emission scenario, the modeled climate-carbon cycle feedback is estimated to cause an additional increase in CO₂ content of between 20 ppmv to 200 ppmv by 2100, which corresponds to an additional global temperature increase of 0.1 °C–1.5 °C (Friedlingstein *et al.*, 2006). The large uncertainty in carbon-climate feedbacks is associated with the different sensitivities of simulated terrestrial carbon cycle processes to changes in climate and atmospheric CO₂ (Friedlingstein *et al.*, 2006; Huntingford *et al.*, 2009). Other important processes, such as nutrient limitations and land use recovery, may further affect terrestrial carbon-climate interactions (Arneeth *et al.*, 2010; Zaehle & Dalmonech, 2011).

In this study, a set of 10 process-based models is tested for their ability to predict current global carbon fluxes (GPP, NPP, & NBP) and their apparent sensitivity to climate variability and rising atmospheric CO₂ concentration. The model ensemble includes: HyLand (Levy *et al.*, 2004), Lund-Potsdam-Jena DGVM (Sitch *et al.*, 2003), ORCHIDEE (Krinner *et al.*, 2005), Sheffield-DGVM (Woodward *et al.*, 1995; Woodward & Lomas, 2004), TRIFFID (Cox, 2001), LPJ-GUESS (Smith *et al.*, 2001), NCAR_CLM4C (Oleson *et al.*, 2010; Lawrence *et al.*, 2011), NCAR_CLM4CN (Oleson *et al.*, 2010; Lawrence *et al.*, 2011), OCN (Zaehle & Friend, 2010), and VEGAS (Zeng *et al.*, 2005b). We compare the model output of NBP with the RLS from Friedlingstein *et al.* (2010) (hereafter FR10). For global climatological GPP we will compare model results with the data-driven model of GPP from Jung *et al.* (2011) (hereafter JU11). The JU11 model is not a direct measurement of GPP, but a statistical model based on the space/time interpolation of flux tower observations using a model tree ensemble (MTE) regression trained with satellite FAPAR and gridded climate fields predictors. Finally, ecosystem controlled warming experiments (six sites) and Free-Air CO₂ Enrichment (FACE) experiments (four sites) are used to test the sensitivity of modeled NPP to individual changes in temperature and CO₂.

Material and methods

Terrestrial carbon cycle models

The 10 carbon cycle models used in this study are briefly described in the Table S1. All models describe surface fluxes of CO₂, water and the dynamics of water and carbon pools in response to change in climate and atmospheric composition. However, the formulation and number of processes primarily responsible for carbon and water exchange differs among models.

Two simulations, S1 and S2, were performed over the period 1860–2009. In S1, models were forced with rising atmospheric CO₂ concentration, while climate was held constant (recycling climate mean and variability from the early decades of the 20th century, e.g., 1901–1920). In S2, models were forced with reconstructed historical climate fields and rising atmospheric CO₂ concentration. All models used the same forcing files, of which historical climate fields were from CRU-NCEP v4 dataset (<http://dods.extra.cea.fr/data/p529viov/cruncep/>) and global atmospheric CO₂ concentration was from the combination of ice core records and atmospheric observations (Keeling & Whorf, 2005 and update). Details of the simulation settings are described in S. Sitch, P. Friedlingstein, N. Gruber, S. Jones, G. Murray-Tortarolo, A. Ahlstrom, S.C. Doney, H. Graven, C. Heinze, C. Huntingford, S. Levis, P.F. Levy, M. Lomas, B. Poulter, N. Viovy, S. Zaehle, N. Zeng, A. Armeth, G. Bonan, L. Bopp, J.G. Canadell, F. Chevallier, P. Ciais, R. Ellis, M. Gloor, P. Peylin, S. Piao, C. Le Quere, B. Smith, Z. Zhu, R. Myneni (submitted). It should be noted that land use change was not taken into account in S1 and S2.

Data-oriented global estimation of GPP

Direct observation of Gross Primary Production (GPP) at the global scale does not exist. Thus, we used a GPP gridded data product from a Model Tree Ensemble (MTE) model-data fusion scheme involving eddy covariance flux tower data, climate, and satellite FAPAR fields (Jung *et al.*, 2011), available during 1982–2008, to compare with modeled GPP. The MTE statistical model employed by JU11 consists of a set of regression trees trained with local GPP estimation from eddy flux NEE measurements with the Lasslop *et al.* (2010) method to separate GPP. In addition, 29 candidate predictors were used covering climate and biophysical variables such as vegetation types, observed temperature, precipitation and radiation, and satellite-derived fraction of absorbed photosynthetic active radiation (FAPAR). The ensemble of the trained regression trees was driven by global fields of predictor variables to derive gridded GPP estimates (Beer *et al.*, 2010). Uncertainty of the GPP estimated from MTE is relatively small, at about ± 6 Pg C yr⁻¹ (Jung *et al.*, 2011). However, this does not consider other sources of uncertainty such as measurement uncertainties of eddy covariance fluxes, of global predictor variables as well as sampling bias driven by unevenly distributed eddy covariance flux sites, with many sites in temperate regions and very few sites in the tropics. As described further below, this dataset should also be used with extreme caution for assessment of interannual variability of GPP.

The 'residual' land sink (RLS)

The RLS of anthropogenic CO₂ during the period 1980–2009 is taken from the Global Carbon Project carbon budget from Friedlingstein *et al.* (2010) and Le Quere *et al.* (2009). It is estimated as a residual of all other terms that compose the global budget of anthropogenic CO₂, as no direct global observation of land carbon balance is available, except for the global forest sink on decadal scale (Pan *et al.*, 2011). The RLS is the sum of fossil fuel, cement and land use change emissions minus the sum of observed atmospheric CO₂ growth rate and modeled ocean sink. The CO₂ emissions from fossil fuel and cement are estimated based on statistics provided by United Nations Energy Statistics (Boden *et al.*, 2012), British Petroleum statistic review of world energy (<http://www.bp.com/productlanding.do?categoryId=6929&contentId=7044622>), and USGS statistics on cement production (Van Oss, 2008). Emissions from land use change (Houghton, 1999) are based on forest area loss national statistics published by the United Nations Food and Agriculture Organization and a book-keeping model (Houghton, 2010) to convert forest area changes into net CO₂ fluxes, including legacy effects of past cohorts of deforested areas. Atmospheric annual CO₂ growth rate is derived from the NOAA/ESRL global cooperative air-sampling network (Conway *et al.*, 1994). The ocean sink of anthropogenic CO₂ is calculated from the average of four ocean carbon cycle models (Le Quere *et al.*, 2009). It is important to note that the net land use source estimate in FR10 is 0.3 Pg C yr⁻¹ lower over 2000–2009 than the previous LUC emission estimate (Le Quere *et al.*, 2009). This lower estimate uses the same Houghton *et al.* model, but takes as input data updated information on forest area change from FAO, TBRFA 2010, instead of the TBRFA 2005. A lower LUC emission estimate results in a lower RLS mean value.

Field ecosystem warming experiment

Data from a harmonized field warming experiment dataset compiled from 124 published articles (Lu *et al.*, 2012) were used to evaluate model performance. To compare with model outputs, available observations of Net Primary Production (NPP) in experimental sites with warming only treatments and the control experiment (no warming) were used in this study. Six sites are located over the temperate and boreal northern hemisphere between 30°N and 70°N with mean annual temperature spanning from -7 °C to 16 °C and mean annual precipitation spanning from 320 mm to 818 mm (Table S2). The magnitude of applied warming ranges from 1 °C to 3.5 °C among different treatments and different sites. These levels of warming are of a magnitude equal or higher than interannual variability in temperature, and so complement comparison of simulations S2 and their testing against data, where for the latter an emphasis might be placed on anomalously warm years. It should be noted that total NPP (both aboveground and belowground NPP) were measured in four of the sites, whereas the other two sites (HARS and Toolik Lake) only measured aboveground NPP.

Free-Air Carbon Dioxide Enrichment (FACE) experiments

Free-Air Carbon Dioxide Enrichment (FACE) experiment provides field experimental data on the response of NPP to elevated CO₂. Four FACE experiments in temperate forest stands provide data for our evaluation (Table S3). NPP was calculated as annual carbon increments in all plant parts plus the major inputs to detritus, litterfall, and fine root turnover. We used data from ORNL FACE Norby *et al.* (2005). But these data are corrected and extended to 2008 (Iversen *et al.*, 2008). Data from young stands in the early stage of sapling development with expanding canopies, and some plots with elevated O₃ at the ASPEN FACE were not included in the dataset, as described by Norby *et al.* (2005). There were in total 21 site-year NPP observations available for our study. Site characteristics and experiment settings in each stand can be found in Table S3, with a more detailed description given in Norby *et al.* (2005). There are no FACE experiments for tropical ecosystems.

Analysis

Response of carbon fluxes to climate variations. We estimate empirically the response of GPP, NPP, and NBP to climate variability (interannual MAT and annual precipitation) over the last three decades using a multiple regression approach Eqn (1):

$$y = \gamma^{\text{int}}x_T + \delta^{\text{int}}x_P + \varepsilon \quad (1)$$

where y is the detrended anomaly of the carbon fluxes GPP, NPP, and NBP from the S2 simulations (i.e., simulations considering change in both climate and atmospheric CO₂ concentration, see section 'Terrestrial carbon cycle models') estimated by each model. Eqn (1) is also fitted to the data-oriented model of GPP (JU11 GPP) and to the RLS values from FR10. The variable x_T is the detrended MAT anomaly, and x_P is the detrended annual precipitation anomaly. The fitted regression coefficients γ^{int} and δ^{int} define the *apparent carbon flux sensitivity* to interannual variations in temperature and precipitation, and ε the residual error term. Note that γ^{int} (or δ^{int}) is the contributive effect of temperature (or precipitation) variations on carbon fluxes, but not the 'true' sensitivities of these fluxes, given that: (i) temperature and precipitation covary over time; and (ii) other climate drivers discarded in Eqn (1), such as solar radiation, humidity, and wind speed may also contribute to the variability of y . The regression coefficients are calculated using maximum likelihood estimates (MLE). The uncertainty in γ^{int} and δ^{int} is obtained from the standard error of the corresponding regression coefficients. Data from 1980 to 2009 were used to quantify the response of carbon fluxes to climate variations, except for GPP where instead the period 1982–2008 was considered to be consistent with the period covered by the JU11 data-oriented estimate. To be consistent with RLS, we first aggregate each grid cell carbon flux into a global mean flux (see SI) and then remove the trend using a least-squares linear fitting method.

Response of carbon fluxes to CO₂ trended over the past 30 years. Two approaches were applied to estimate the response of carbon fluxes to CO₂ (β). In the first approach, β was estimated based on S1 simulations (i.e., the simulations where the only driver of NPP and NBP is the increase of atmospheric CO₂) using Eqn (2):

$$\beta = \frac{\Delta F}{\Delta \text{CO}_2} \quad (2)$$

where, ΔF is the difference of average carbon fluxes between the last and the first 5 years of the S1 simulation, and ΔCO_2 is the corresponding change in atmospheric CO₂ concentration. To estimate the uncertainty of β , we also calculated an ensemble of β values over the study period by randomly selecting a different year over the first and last 5-year period.

In the second approach, we used a multiple regression approach Eqn (3) to estimate β for RLS, or for JU11 GPP, and for each model carbon flux from simulation S2 (both climate and CO₂ change).

$$y = \beta \text{CO}_2 + a \text{Tmp} + b \text{Prpc} + c + \varepsilon \quad (3)$$

where, y is the carbon flux of each model (NBP or GPP) from S2, or the observed RLS from FR10, and CO₂, Tmp, and Prpc are the atmospheric CO₂ concentration, MAT and annual precipitation, respectively. β , a , b , and c are regression coefficients, and ε is the residual error term. The regression coefficients are calculated using maximum likelihood estimates (MLE). Eqn (3) attributes the time series of y to what we consider as the dominant drivers of change i.e., temperature, precipitation, and CO₂. However, we do recognize that changes of other meteorological forcing might influence y as well. Those confounding drivers are implicitly accounted for in the value of the regression coefficients. Confounding drivers are land use, forest demography, nitrogen deposition, solar radiation, humidity, and wind speed, which modulate the trend of RLS time series in addition to the assumed CO₂ driver. Therefore, the inferred value of β from Eqn (3) should be treated with caution. In general, a and b indicate the contributive effect of temperature (resp. precipitation) variations on the carbon fluxes variations (Fig. S1). The period 1980–2009 is used to estimate the carbon fluxes sensitivities to climate and CO₂, except for GPP where the period considered is 1982–2008.

Temperature sensitivities of vegetation productivity derived warming experiment. For warming experiments field measurements, the sensitivity of NPP to an applied change in temperature (generally stepwise), is estimated as the ratio of the relative difference between NPP in warmed minus control plots to the applied warming magnitude. The estimated temperature sensitivity at each experimental site is then compared with the ratio of $\gamma_{NPP}^{\text{int}}$ estimated from model simulations and with the multiple regression method Eqn (1) to the 30-year average NPP. This ratio is hereafter called $R_{\gamma_{NPP}^{\text{int}}}$. The model output is sampled at the grid point containing the experimental site. In addition, we also extract modeled sensitivities in 'climate analogue' grid points where the mean annual temperature differs by less than 1 °C and mean annual precipitation by less than 50 mm from the conditions at each experimental

site. Only analogue grid points with the same dominant vegetation type as observed at each experimental site are retained, e.g., for grassland warming sites; all grid points with grassland cover of less than 50% are excluded. As models do not explicitly represent wetland processes, we grouped wetland with grasslands. Using a similar approach, we estimated the sensitivities of NPP to rising atmospheric CO₂ concentration from the FACE sites and the relative response of NPP to CO₂ ($R\beta_{NPP}$, the ratio of β_{NPP} estimated by Eqn (2) to the 30-year average NPP in each model).

Due to the normalization of the response of NPP to temperature and/or CO₂, we cannot make quantitative statements about the nature of the model-data agreement. Both, the stepwise nature of the experiment and the magnitude of the perturbation may induce nonlinear effects in the ecosystems that cannot (and should not) be reproduced by ecosystem models simulating the consequences of a gradual and less pronounced perturbation over the last three decades. In particular, because of the saturating effect of CO₂ on leaf level photosynthesis, we expect to see a larger relative effect of CO₂ on photosynthesis when evaluating the increase from 338 to 386 ppm than the response from field experiments elevating CO₂ concentration from about 360–550 ppm.

Vegetation productivity

GPP estimation

Global terrestrial GPP averaged across the 10 models is 133 ± 15 Pg C yr⁻¹, ranging from 111 ± 4 Pg C yr⁻¹ (\pm SD of GPP over the three decades) in SDGVM to 151 ± 4 Pg C yr⁻¹ in ORCHIDEE and CLM4C. The higher estimates are consistent with the inferred estimate from ¹⁸OCO in the atmosphere (Welp *et al.*, 2011), although this high value is also subject to uncertainty and in contrast with earlier studies (Ciais *et al.*, 1995; Beer *et al.*, 2010). The JU11 GPP product derived from eddy covariance flux towers, generally gives a lower estimate of GPP than the majority of the processed-based models (Fig. 1), particularly in temperate regions (Fig. S2b). At the global scale, the magnitude of GPP (113 ± 3 Pg C yr⁻¹) in LPJ-GUESS is close to JU11 (118 ± 1 Pg C yr⁻¹). However, this result should be viewed with caution, since a similar global average GPP can mask compensation of biases, for instance, between tropical and nontropical regions. As shown by Fig. S2, the LPJ-GUESS simulation has a low bias of GPP in tropical regions compared with JU11 (68% of JU11), compensated by a high bias in nontropical regions. This is also illustrated in the cumulative frequency distribution of GPP (Fig. S3). Few grids in the LPJ-GUESS simulation have GPP larger than 2000 g C m⁻² yr⁻¹, whereas JU11 and eight of the other nine models (except SDGVM) show that at least 10% of the global grids have GPP larger than 2000 g C m⁻² yr⁻¹.

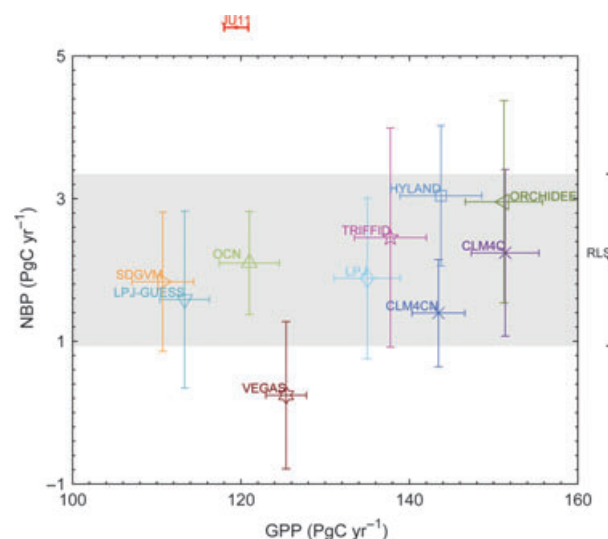


Fig. 1 The magnitude of global Gross Primary Production (GPP) and global Net Biome Productivity (NBP) estimated by the 10 carbon cycle models. *x*-axis indicates mean annual global GPP during 1982–2008 with error bars showing standard deviation of the interannual variations. *y*-axis indicates mean annual global NBP during 1980–2009 with error bars showing standard deviation of the interannual variations. The red line shows global GPP estimated by a data-driven model tree ensemble approach (JU11, Jung *et al.*, 2011), while black lines shows global Residual Land Sink (RLS) (Friedlingstein *et al.*, 2010). Global RLS is estimated as the difference between CO₂ emissions (from fossil fuel combustion and land use change) and carbon storage change in the atmosphere (atmospheric CO₂ growth rate) and in the oceans (model simulated ocean carbon sink) (Friedlingstein *et al.*, 2010). The 10 carbon cycle models include Community Land Model 4C (CLM4C), Community Land Model 4CN (CLM4CN), HYLAND, Lund-Potsdam-Jena (LPJ), LPJ-GUESS, O-CN (OCN), ORCHIDEE, Sheffield-DGVM (SDGVM), TRIFFID and VEGAS.

At the global scale, the correlation of interannual GPP variations among the different models is much higher than that of any model with JU11 as shown by Fig. 2a. JU11 GPP is estimated from satellite and eddy covariance flux tower measurements. The flux tower sites are mainly distributed in northern temperate regions (mainly forest). Hence, a larger sampling uncertainty is associated with JU11 for GPP outside this northern region. This is of importance because tropical ecosystems are largely driving the interannual variability in the carbon cycle (Denman *et al.*, 2007). Interestingly, the lowest correlation between GPP from models and JU11 is found in tropical regions (Fig. S4c) perhaps due to the fewer eddy covariance flux sites available to create the JU11 gridded product. Furthermore, the interannual standard deviation of GPP is found to be substantially higher in the 10 process models than in

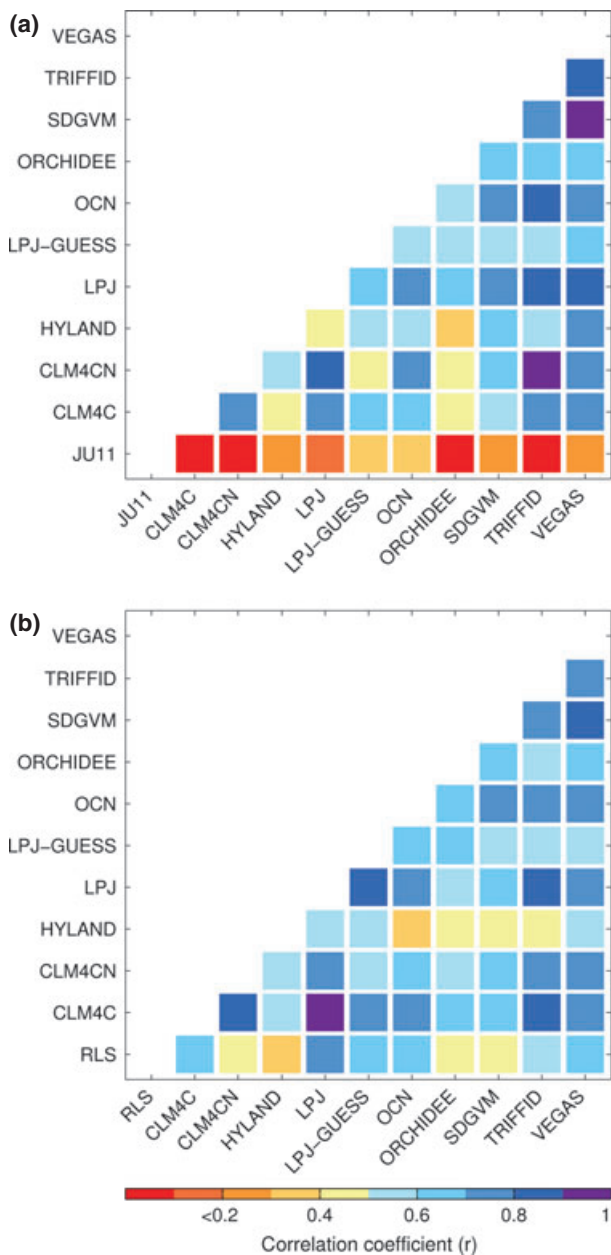


Fig. 2 Color-coded correlation matrixes for global GPP estimated by the 10 carbon cycle models and a data-driven model tree ensemble approach (JU11, Jung *et al.*, 2011) and global NBP estimated by the 10 carbon cycle models and global Residual Land Sink (RLS) (Friedlingstein *et al.*, 2010). The correlation matrixes display (a) correlation coefficient in pairs among detrended GPP anomalies estimated by the different approaches during 1982–2008. (b) correlation coefficient in pairs among detrended NBP anomalies estimated by different models and RLS during 1980–2009. Model abbreviations are the same as in Figure 1.

JU11 (compare error bars in Fig. 1a), particularly over tropical regions (Fig. S2c). This leads us to make the hypothesis that the GPP interannual variability is

undersampled in JU11 and hence systematically lower than the interannual variability simulated by the models. This hypothesis is further discussed in the next section.

Response of GPP to temperature variations (γ_{GPP}^{int})

At the global scale, the model output suggests that interannual variation in global GPP is not significantly correlated with temperature (all variables detrended), as can be seen from the large differences in the magnitude and even in the sign of γ_{GPP}^{int} (Fig. 3a) due to the different sensitivity values over different regions (Fig. S6). In the tropical regions, all models have a negative apparent sensitivity to temperature γ_{GPP}^{int} (-2.2 ± 1.2 Pg C yr⁻¹ °C⁻¹ or $-2.9 \pm 1.4\%$ °C⁻¹; significant for seven of 10 models). JU11 has a positive γ_{GPP}^{int} (0.4 ± 0.7 Pg C yr⁻¹ °C⁻¹ or $0.6 \pm 1.0\%$ °C⁻¹, $P > 0.05$) (Fig. S6c). JU11's GPP response to temperature variability over tropical regions, however, may be considered rather uncertain, as satellite FAPAR used by JU11 for spatial–temporal interpolation of GPP distribution between flux tower locations is often contaminated by cloudiness (Myneni *et al.*, 1997). Furthermore, JU11 trained their MTE using *spatial gradients* among different sites (there are few long series) and then used the derived relationship to extrapolate to *temporal interannual* gradients. This assumes that spatial and interannual sensitivity of GPP to climate are the same, which may be not correct. Measurements of annual tree growth in tropical forests have shown negative correlation with temperature (Clark *et al.*, 2003, 2008). This result is supported by short-term leaf level measurements in tropical forests, which indicate a decrease in net carbon assimilation at higher temperature (Tribuzy, 2005; Doughty & Goulden, 2008). This negative response of vegetation productivity to MAT variability may arise from the fact that tropical forests already operate near to a high-temperature optimum threshold above which vegetation photosynthesis declines sharply (Corlett, 2011).

In boreal regions, vegetation growth is limited by temperature which controls (among other variables) the length of the growing season. This implies that rising MAT causes an extension of the growing season, and induces an increase in GPP (Piao *et al.*, 2007; Richardson *et al.*, 2010) during warm years. It has been suggested that rising temperature is currently enhancing vegetation growth in boreal regions (Lucht *et al.*, 2002; Piao *et al.*, 2006, 2009a; Wang *et al.*, 2011) except in regions affected by summer drought, during the analysis period, such as parts of Alaska (Beck *et al.*, 2011). All the models show significant positive relationship ($P < 0.05$) between boreal GPP and MAT

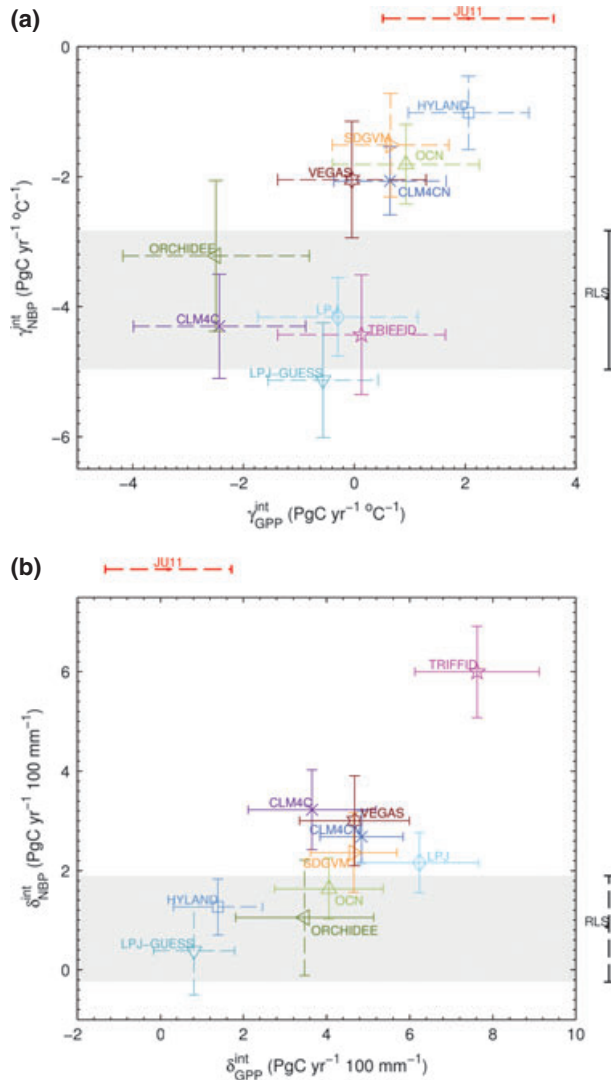


Fig. 3 The response of global Gross Primary Production (GPP), global Net Biome Production (NBP) and global Residual Land Sink (RLS) to (a) interannual variation in temperature (γ_{GPP}^{int} , γ_{NBP}^{int} and γ_{RLS}^{int} , respectively) and (b) interannual variation in precipitation (δ_{GPP}^{int} , δ_{NBP}^{int} and δ_{RLS}^{int} , respectively). γ_{GPP}^{int} and δ_{GPP}^{int} are estimated using Eqn (1) with data during 1982–2008. γ_{NBP}^{int} , δ_{NBP}^{int} , γ_{RLS}^{int} and δ_{RLS}^{int} estimated using Eqn (1) with data during 1980–2009. Gray area indicates the standard error of γ_{RLS}^{int} and δ_{RLS}^{int} . Error bars show standard error of the sensitivity estimates. Dashed error bars in both (a) and (b) indicate the estimated sensitivity from the regression approaches are statistically insignificant ($P > 0.05$). The red line shows the 1σ range of β_{GPP} estimated by JU11's GPP products using Eqn (3). Model abbreviations are the same as in Figure 1.

with an average γ_{GPP}^{int} of $0.8 \pm 0.3 \text{ Pg C yr}^{-1} \text{ } ^\circ\text{C}^{-1}$ (or $4.5 \pm 1.5\% \text{ } ^\circ\text{C}^{-1}$). This apparent temperature sensitivity is close to the γ_{GPP}^{int} diagnosed from the GPP of JU11 ($0.9 \pm 0.3 \text{ Pg C yr}^{-1} \text{ } ^\circ\text{C}^{-1}$ or $4.7 \pm 1.5\% \text{ } ^\circ\text{C}^{-1}$) (Fig. S6a).

In temperate regions, the response of GPP to MAT depends partly on the balance between the positive effect of warming through extending the growing season in spring and possibly in autumn and the negative effect of warming through enhanced soil moisture stress in summer. Some recent work also suggests that the photoperiod may limit GPP (Bauerle *et al.*, 2012). At the regional scale, most models (except CLM4CN and HYLAND) and JU11 show a nonsignificant interannual correlation between MAT and GPP (Fig. S6b).

Comparison with the field warming experiments

Figure 4 shows the spatial distribution of $R\gamma_{NPP}^{int}$ (the ratio of γ_{NPP}^{int} to the 30-year average NPP of each model) averaged across the 10 models. Similar to the regional scale analyses of γ_{GPP}^{int} above, we obtained a positive (resp. negative) interannual correlation between MAT and NPP in boreal (resp. tropical) regions. We then compared the simulated $R\gamma_{NPP}^{int}$ against the relative sensitivity observed in field warming experiments (note only distributed over the northern hemisphere). Field warming experiments show that a step increase in temperature generally increases NPP (after 4 years of warming on average) across most sites, except at the Haibei Alpine Research Station (in the Tibet Plateau) where rising temperature significantly decreased aboveground NPP by $-8\% \text{ } ^\circ\text{C}^{-1}$ (Fig. 4). The sign of $R\gamma_{NPP}^{int}$ at Haibei is correctly captured by six of 10 models (Fig. 4). One can also see in Fig. 4 that models tend to predict smaller $R\gamma_{NPP}^{int}$ values than observed at the warming experiment temperate sites, particularly at Jasper Ridge Global Change Experiment (JRGCE), Kessler's Farm Field Laboratory (KFFL), Alborn (Minnesota 2), and Duolun. One can assume that this may be because in the grid points containing these sites, annual precipitation used in model forcing is less than actual precipitation at field sites (by 15% at Jasper Ridge Global Change Experiment, 8% at Kessler's Farm Field Laboratory, 46% at Toivola and Alborn, and 17% at Duolun). The results of two field warming experiment sites in Minnesota, USA (47°N , 92°W) have shown that the wetter site (annual precipitation of 762 mm) has a much higher NPP sensitivity to warming ($12\text{--}22\% \text{ } ^\circ\text{C}^{-1} \text{ yr}^{-1}$) than the drier site (annual precipitation of 497 mm, $-3\text{--}6\% \text{ } ^\circ\text{C}^{-1} \text{ yr}^{-1}$) (Fig. 4), implying that average climatic conditions (in particular through soil moisture availability) regulate the response of NPP to temperature. To minimize the effect of biases in the climate drivers, we also extracted $R\gamma_{NPP}^{int}$ at 'climate analogue' grid points where the mean annual temperature differs by less than $1 \text{ } ^\circ\text{C}$ and mean annual precipitation by less than 50 mm from the conditions at each experimental site. As shown in Fig. 4, however, the model

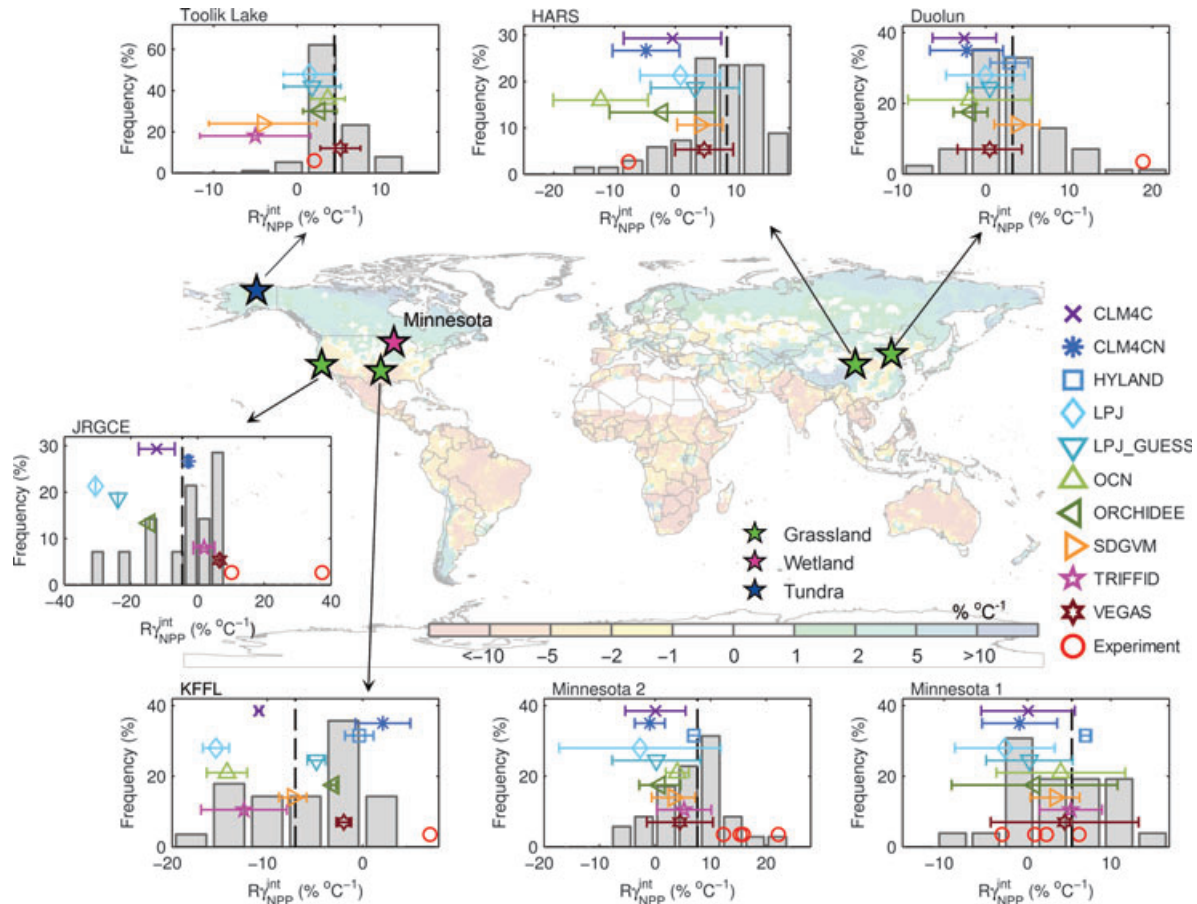


Fig. 4 Comparisons of observed relative response of Net Primary Production (NPP) to temperature change in warming experiments (Lu *et al.*, 2013, Table S1) and estimated relative response of NPP to interannual variation in temperature ($R_{\gamma_{NPP}}^{int}$, the ratio of γ_{NPP}^{int} to 30-year average NPP) by 10 models for the period of 1980–2009. The gray histogram at each site shows the frequency distribution of $R_{\gamma_{NPP}}^{int}$ according to the ensemble of 10 model simulations at the grid containing the experiment site and at model grids with grassland dominant land cover (grassland vegetation more than 50% according to GLC land cover map, changing the threshold of grassland percentage from 50% to 70% only induce small change in the frequency distribution of $R_{\gamma_{NPP}}^{int}$ and with similar climate to the experiment site (the difference in mean annual temperature less than 1 °C and difference in mean annual precipitation less than 50 mm). The mean of model estimated $R_{\gamma_{NPP}}^{int}$ is shown in dashed black line. Model estimates at the grid cell of the experiment site are shown using model-specific mark and color with horizontal error bars showing standard error of $R_{\gamma_{NPP}}^{int}$ estimated by the same model in the ensemble of this grid and grids with grassland dominant land cover and showing similar climate. The position of model-specific mark in the vertical axis only represents alphabetical order of model abbreviations. Observed relative temperature sensitivities of NPP in different plots or different time period in the same site, if reported, are shown separately in red circles. As belowground NPP was not measured in HARS and Toolik Lake, experiment observed temperature sensitivities of NPP at the two sites were based on aboveground NPP measurements. The background color map shows spatial distribution of average of $R_{\gamma_{NPP}}^{int}$ from 10 carbon cycle models. Pentagrams in the color map show locations of experiment sites. Model abbreviations are the same as in Figure 1.

estimated $R_{\gamma_{NPP}}^{int}$ at JRGCE, KFFL, Minnesota 2, and Duolun, is still systematically lower than observation. This suggests that the different forcing may be not the primary reason for the mismatch between models and observations. A recent study comparing model simulations driven by site-level climate forcing and by gridded climate forcing supports this conclusion, through the fact that model structure, rather than climate forcing, remained the main limitation for improving model-site data comparison (B.M. Raczka, K. Davis, D. Huntzinger,

R. Neilson, B. Poulter, A. Richardson, J. Xiao, I. Baker, P. Ciais, F. Keenan, B. Law, W. Post, D. Ricciuto, K. Schaefer, H. Tian, H. Tomellieri, N. Viovy, submitted).

In addition, it should be noted that the methods we used to quantify the response of NPP to temperature change in models (interannual variability) and in field warming experiments (multiyears treatments have a higher amplitude of stepwise warming than the interannual range of natural variability, and no covariate precipitation change) are different, which may cause

inconsistencies in evaluating models. Even at the same site, the magnitude of the temperature sensitivity of NPP depends on the magnitude of warming. For example, field warming experiments at the drier site in Minnesota, USA (47°N, 92°W) show that temperature sensitivity of NPP for a step 2 °C warming (1–6% yr⁻¹) is larger than that for a step 3 °C warming (–3–2% yr⁻¹). Furthermore, R_{NPP}^{int} of processed-based models does not consider local heterogeneity of environmental conditions and land cover, and local biogeophysical feedbacks with the atmosphere (e.g., Long *et al.*, 2006). This spatial scale mismatch adds uncertainty to model evaluation using warming experiment sites. For instance, the temperature sensitivity of NPP derived from the warming experiment at the two Minnesota sites (47°N, 92°W) that are located in the same grid point of models, varies from –3% °C⁻¹ to 22% °C⁻¹, which is a larger range than that predicted by the models over the corresponding grid point (from –2.7% °C⁻¹ to 6.1% °C⁻¹). In addition, models may not fully represent ecosystem-level mechanisms underlying NPP responses to warming in experiments, such as warming-induced changes in nutrient availability, soil moisture, phenology, and species composition (Luo, 2007). Overall, the inconsistency of the response of NPP to temperature change between models and field warming experiments should be addressed by further studies, for instance, running the same models with site observed forcing data and vegetation, and soil parameters.

Response of GPP to precipitation variations $\delta_{GPP}^{\text{int}}$

Over the past few decades, many regions experienced drought, which has a negative effect on vegetation productivity (Zhao & Running, 2010; for the globe; Angert *et al.*, 2005 and Zeng *et al.*, 2005a for the Northern Hemisphere; Ciais *et al.*, 2005 for Europe; Zhang *et al.*, 2010 for North America; Poulter *et al.*, 2010 for Amazonia, Mcgrath *et al.*, 2012; for Australia, Wang *et al.*, 2010 for China). Droughts that occurred from 1998 to 2002 in the northern hemisphere midlatitudes, for example, led to an estimated reduction in vegetation NPP by 5% compared with the average of the previous two decades (Zeng *et al.*, 2005a). Although individual drought events cannot be attributed to anthropogenically induced climate change, there is a concern that a general situation of more extreme weather events is emerging, including the potential for alteration to the global hydrological cycle. Over the northern hemisphere, all models have a positive $\delta_{GPP}^{\text{int}}$. However, the interannual correlation between GPP and precipitation was found to be not significant for JU11, HYLAND, LPJ-GUESS, and VEGAS in boreal regions (Fig. S7a), and JU11, HYLAND in northern temperate regions (Fig. S7b).

There has been much discussion in the literature about the impact of drought on vegetation growth and mortality in tropical regions (Nepstad *et al.*, 2004; Phillips *et al.*, 2009, 2010; Da Costa *et al.*, 2010). A rainfall exclusion experiment in an east-central Amazonian rainforest at Tapajos showed that a 50% reduction in precipitation led to a 25% reduction in vegetation NPP over the first 2 years of the experiment (Nepstad *et al.*, 2002). It has been suggested that spatial GPP variability in 30% of tropical forest and in 55% of tropical savannahs and grasslands is primarily correlated with the precipitation (Beer *et al.*, 2010). All models indeed show a positive correlation of GPP with annual precipitation over tropical regions (not significant in JU11 and HYLAND), but the magnitude of $\delta_{GPP}^{\text{int}}$ differs among models with TRIFFID and LPJ having the largest $\delta_{GPP}^{\text{int}}$ (about 2.2 ± 0.4 Pg C yr⁻¹ per 100 mm or $2.8 \pm 0.5\%$ per 100 mm for TRIFFID, and 1.8 ± 0.4 Pg C yr⁻¹ per 100 mm or $2.7 \pm 0.5\%$ per 100 mm for LPJ) (Fig. S7c). The average of tropical $\delta_{GPP}^{\text{int}}$ across the 10 models is 1.4 ± 0.5 Pg C yr⁻¹ per 100 mm (or $1.8 \pm 0.7\%$ per 100 mm), which is three times larger than $\delta_{GPP}^{\text{int}}$ of the JU11 data-oriented GPP (0.5 ± 0.3 Pg C yr⁻¹ per 100 mm or $0.6 \pm 0.4\%$ per 100 mm).

Overall, at the global scale, $\delta_{GPP}^{\text{int}}$ averaged across the 10 models is 4.1 ± 2.0 Pg C yr⁻¹ per 100 mm (or $3.1 \pm 1.5\%$ per 100 mm) (Fig. 3b). Among the 10 models, eight exhibit significant positive correlations between global GPP and annual precipitation (all variables detrended). Considering that global GPP was not correlated with MAT in any of the models (see section ‘Response of GPP to temperature variations’), we conclude that interannual variation in GPP is more closely controlled by precipitation rather than by temperature (Piao *et al.*, 2009b; Jung *et al.*, 2011) in the models parameterizations. The TRIFFID model has the highest $\delta_{GPP}^{\text{int}}$ (7.6 ± 1.5 Pg C yr⁻¹ per 100 mm or $5.5 \pm 1.1\%$ per 100 mm) as seen in Fig. 3b. Differences in simulated land cover between models, in addition to structural sensitivities (i.e., sensitivity of stomata to soil moisture) may also explain the variability among models, particularly in arid and temperate regions (Poulter *et al.*, 2011).

Response of vegetation productivity to CO₂

According to the results of simulation S1 driven by atmospheric CO₂ only, model results consistently indicate that rising atmospheric CO₂ concentration increased NPP by 3–10% with an average of 7% over the past three decades (for a 48 ppm CO₂ increase) (or 0.05–0.2% ppm⁻¹ with the average of 0.16% ppm⁻¹). This relative response of NPP to CO₂ (R_{NPP}) is slightly larger than the sensitivity derived from FACE

elevated CO₂ experiments. This result is expected because of the saturating effect of CO₂ on photosynthesis. Norby *et al.* (2005) analyzed the response of NPP to elevated CO₂ in four FACE experiments in temperate forest stands and concluded that the enhancement of NPP due to elevated CO₂ (about 180 ppmv) was of about 23% (or 0.13% ppm⁻¹). When comparing the results from the four FACE experiments with model simulations at the corresponding sites and climatic condition, however, we found that the models underestimated CO₂ fertilization effect on NPP at the ASPEN FACE site, but overestimated it at the Duke and ORNL FACE sites (Fig. 6). The study of Hickler *et al.* (2008) suggested that the currently available FACE results are not applicable to vegetation globally as there is large spatial heterogeneity of the positive effect of CO₂ on vegetation productivity across the global land surface. Hence, we do not present the FACE values in global plot Fig. 5a. As shown in Fig. 6, the modeled response of NPP to CO₂ is generally larger in drier regions. Among the four FACE experimental sites, a largest CO₂ fertilization effect of NPP was also found in the driest (ASPEN FACE) site (Fig. 6 and Table S3). This NPP enhancement could be due to the additional saving of soil moisture induced by elevated CO₂ on stomatal closure (i.e., increased water use efficiency of plants in water limited regions).

It has been suggested that the CO₂ fertilization effect on vegetation productivity may be overestimated because models ignore N limitations (Hungate *et al.*, 2003; Bonan & Levis, 2010; Zaehle *et al.*, 2010). As in Bonan & Levis, 2010, we find that, for CLM4, β_{GPP} in CLM4CN that considers C–N interaction and N limitations is indeed lower than that estimated in the CLM4C without C–N interaction (Fig. 5a). In boreal regions, β_{GPP} of CLM4CN (2.2 ± 1.4 Pg C yr⁻¹ per 100 ppm or $12 \pm 8\%$ per 100 ppm) is only about half of CLM4C estimated β_{GPP} (4.4 ± 1.5 Pg C yr⁻¹ per 100 ppm or $21 \pm 7\%$ per 100 ppm). As noted previously (Zaehle & Dalmonech, 2011), there is a difference in the extend of N limitation on global carbon cycling between CLM4C-N and OCN, although both of them have N limitations on GPP. OCN predicts a relatively high β_{GPP} , particularly in tropical regions (12.7 ± 1.6 Pg C yr⁻¹ per 100 ppm or $18 \pm 2\%$ per 100 ppm), which is two times larger than that estimated by CLM4CN (6.6 ± 1.2 Pg C yr⁻¹ per 100 ppm or $7 \pm 1\%$ per 100 ppm) (Fig. S9c).

According to Eqn (3), the GPP data-driven product of JU11 shows only a weak sensitivity to CO₂ at the global scale (Fig. 5a), even though satellite data used to drive the empirical model of Jung *et al.* (2011) include a greening trend whose spatial pattern can be partly accounted for by rising CO₂ (Piao *et al.*, 2006). Furthermore, the model results show that β_{GPP}

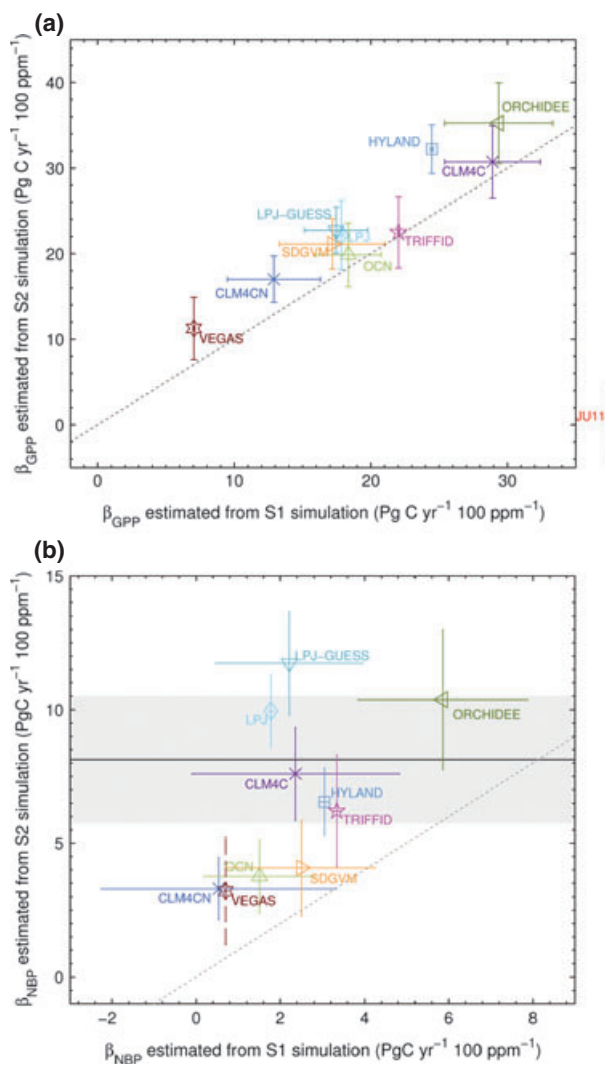


Fig. 5 The response of global Gross Primary Production (GPP), global Net Biome Productivity (NBP), and global Residual Land Sink (RLS) to rising atmospheric CO₂ concentration (β_{GPP} , β_{NBP} and β_{RLS} , respectively). (a) β_{GPP} estimated by the two approaches. *x*-axis indicates β_{GPP} estimated by Eqn (2) using simulation S1, while *y*-axis indicates β_{GPP} estimated by Eqn (3) using simulation S2 with data during 1982–2008. (b) β_{NBP} estimated by two approaches. *x*-axis indicates β_{NBP} estimated by Eqn (2) using simulation S1, while *y*-axis indicates β_{NBP} estimated by Eqn (3) using simulation S2 with data during 1980–2009. Error bars show standard error of the sensitivity estimates. The solid black line shows β_{RLS} estimated by Eqn (3). Gray area shows the standard error of the β_{RLS} . Dashed error bars in both (a) and (b) indicate the estimated sensitivity from the regression approaches are statistically insignificant ($P > 0.05$). Model abbreviations are the same as in Figure 1.

derived from simulations S2 (with both climate change and rising atmospheric CO₂) from Eqn (3) are generally larger than β_{GPP} from simulation S1 which only consider rising atmospheric CO₂ concentration

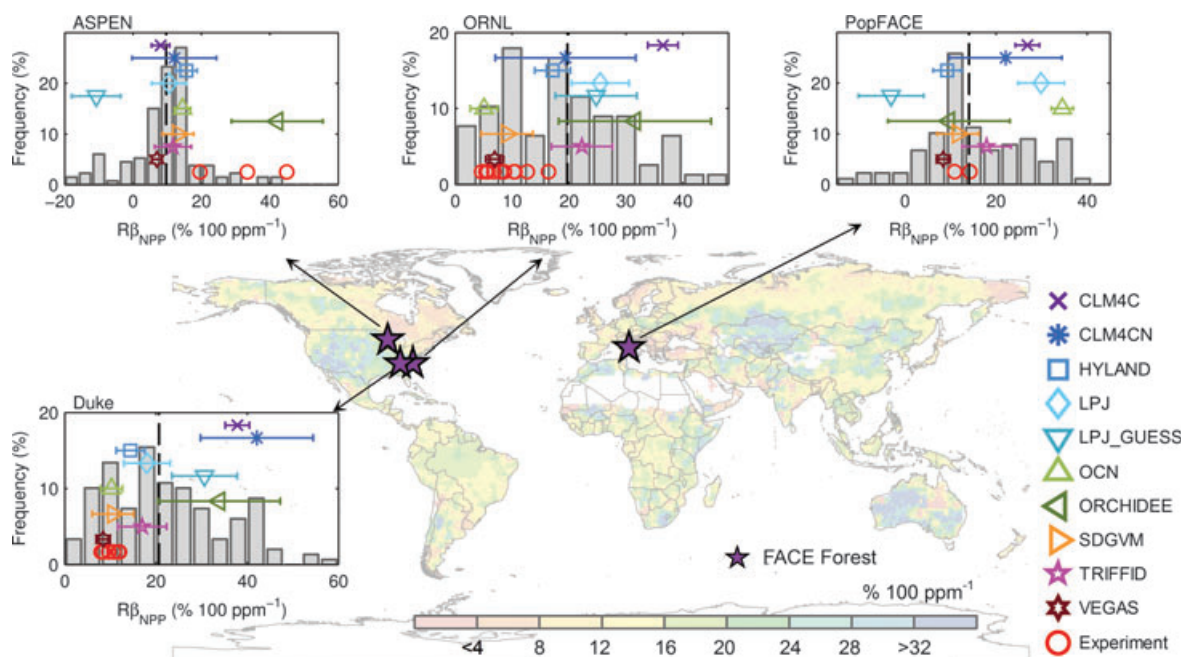


Fig. 6 Comparison of the observed relative response of Net Primary Production (NPP) to rising atmospheric CO₂ concentration in the Free Atmospheric CO₂ Enrichment (FACE) experiment sites (Table S2) and estimated relative response of NPP to rising atmospheric CO₂ ($R\beta_{NPP}$, the ratio of β_{NPP} estimated by the Eqn (2) to 30-year average NPP) by 10 models for the period 1980–2009. The gray histogram at each site shows the frequency distribution of $R\beta_{NPP}$ according to the ensemble of 10 model simulations at the grid containing the experiment site and at model grids with forest dominant land cover (forest vegetation more than 50% according to GLC 2000 land cover map, changing the threshold of forest percentage from 50% to 70% only induce small change in the frequency distribution of $R\beta_{NPP}$) and with similar climate to the experiment site (the difference in mean annual temperature less than 1 °C and difference in mean annual precipitation less than 50 mm). The mean of the model estimated $R\beta_{NPP}$ is shown in dashed black line. Model estimates at the grid containing the experiment site are shown using model-specific symbol and color with horizontal error bars showing standard error of the $R\beta_{NPP}$ estimated by the same model in the ensemble of this grid and grids with forest as the dominant land cover having similar climate. The position of model-specific mark in the vertical axis only represents alphabetical order of model abbreviations. Observed NPP response to rising atmospheric CO₂ at different year at the same site are shown separately in red circles. The background color map shows spatial distribution of $R\beta_{NPP}$ estimated from the average NPP of the 10 carbon cycle models. Solid pentagrams in the map show locations of the FACE forest sites. Model abbreviations are the same to Figure 1.

(Fig. 5a). This is particularly true in the tropical regions (Fig. S9c). This may be partly because the mean climate in the early decades of the 20th century for S1 simulation is wetter than that in the last decades of the 20th century for S2 in the tropical regions (IPCC, 2007), or indicate that the linear regression approach does not replicate the intricate nonlinear complexity of the global carbon cycle.

Net biome productivity

NBP estimation

Global NBP is not significantly correlated with the GPP across the 10 models ($R = 0.48$, $P = 0.16$) (Fig. 1), suggesting that models predicting a larger GPP do not necessarily translate into larger NBP. The standard deviation (SD) of NBP across the 10 models is 2.0 Pg C yr^{-1} , which is smaller than that of GPP ($14.9 \text{ Pg C yr}^{-1}$).

The ensembles model average NBP (all without land use change) during the period 1980–2009 is $2.0 \pm 0.8 \text{ Pg C yr}^{-1}$, which is very close to the RLS of $2.1 \pm 1.2 \text{ Pg C yr}^{-1}$. However, there are large differences among different models, with NBP ranging from $0.24 \pm 1.03 \text{ Pg C yr}^{-1}$ (VEGAS) to $3.04 \pm 0.98 \text{ Pg C yr}^{-1}$ (HYLAND) (Fig. 1). The smaller NBP of VEGAS is related to the net tropical carbon source produced by this model ($-0.12 \pm 0.9 \text{ Pg C yr}^{-1}$). In contrast, the other nine models (in absence of land use) produce a net sink of $1.13 \pm 0.44 \text{ Pg C yr}^{-1}$ on average (Fig. S2c), explaining 54% of global RLS.

In addition, for analysis of the interannual variability in modeled global NBP from 1980 to 2009, the models show generally a good agreement of NBP variability with the observed variability in the RLS ($P < 0.05$) (Fig. 2b). All models show that SD of interannual variation in NBP (average of $1.1 \pm 0.3 \text{ Pg C yr}^{-1}$) is smaller than that of GPP (average of $3.8 \pm 0.8 \text{ Pg C yr}^{-1}$) due

to the strong coupling causing a positive correlation between ecosystem respiration and GPP in the model ($P < 0.05$). Interestingly, for NBP variability, CLM4CN has a lower correlation with RLS than CLM4C (Fig. 2b), implying that in this particular model, incorporation of the nitrogen cycle does not improve the simulation of interannual variability; this may reflect model structural problems in describing processes controlling C–N interactions (Bonan & Levis, 2010). Note, however, that a dampening of the interannual variability in the carbon cycle is not a general feature of nitrogen dynamics (Zaehle *et al.*, 2010). In addition, at the regional scale, the correlation of interannual NBP among different models is higher in the tropical regions than that in nontropical regions (Fig. S5).

Response of NBP to temperature variations (γ_{NBP}^{int})

Direct observational evidence for a positive feedback of the terrestrial carbon cycle to warming is limited (Scheffer *et al.*, 2006; Cox & Jones, 2008; Frank *et al.*, 2010). Applying the regression of Eqn (1) to RLS time series defines an ‘observed’ contributive effect of temperature variations on the RLS variations (γ_{RLS}^{int}) of -3.9 ± 1.1 Pg C yr⁻¹ °C⁻¹ (Fig. 3a). This apparent effect is larger than, but within the uncertainty range of γ_{NBP}^{int} in the 10 models (-3.0 ± 1.5 Pg C yr⁻¹ °C⁻¹). Except for HYLAND and SDGVM, eight of 10 models show significant negative correlation between NBP and MAT. But γ_{NBP}^{int} varies among models from -1.0 ± 0.6 Pg C yr⁻¹ °C⁻¹ in HYLAND to -5.1 ± 0.9 Pg C yr⁻¹ °C⁻¹ in LPJ-GUESS. These differences in γ_{NBP}^{int} across 10 models mainly depend on model differences in the response of GPP to temperature ($R = 0.63$, $P = 0.05$), rather than response of respiration to temperature ($R = 0.44$, $P > 0.05$). Furthermore, the contribution of fire to the γ_{NBP}^{int} is also limited (Fig. S8a). The value of γ_{NBP}^{int} in CLM4CN (-2.1 ± 0.5 Pg C yr⁻¹ °C⁻¹) is only half of that in CLM4C (-4.3 ± 0.8 Pg C yr⁻¹ °C⁻¹), which may be partly because during warmer years, increased soil nitrogen mineralization and availability may promote vegetation growth (Melillo *et al.*, 2002). However, γ_{NBP}^{int} from CLM4C is closer to the observed γ_{RLS}^{int} than for CLM4CN.

The negative value of global γ_{NBP}^{int} is mainly due to negative NBP anomalies (abnormal CO₂ source to the atmosphere) occurring during warm years over tropical regions (Fig. S6c). All models show statistically significant interannual correlation of NBP with MAT in the tropical regions ($R < 0.05$), and an average γ_{NBP}^{int} of -3.0 ± 1.2 Pg C yr⁻¹ °C⁻¹. Compared with tropical regions, other regions have a smaller γ_{NBP}^{int} (Fig. S6). In the boreal zone, there are large differences in the magnitude and even in the sign of γ_{NBP}^{int} among models. For example, LPJ, LPJ-GUESS, and TRIFFID have a γ_{NBP}^{int}

of -0.37 ± 0.13 Pg C yr⁻¹ °C⁻¹, -0.53 ± 0.19 Pg C yr⁻¹ °C⁻¹, and -0.29 ± 0.1 Pg C yr⁻¹ °C⁻¹, respectively, but VEGAS has a positive γ_{NBP}^{int} of 0.23 ± 0.08 Pg C yr⁻¹ °C⁻¹ (Fig. S6a) due to its highest γ_{GPP}^{int} (Fig. S6a). Those model differences for γ_{NBP}^{int} in the boreal zone and the consistency in the sign of γ_{NBP}^{int} over tropical zone between models can explain why models agree more on the interannual variation in tropical NBP than on the interannual variations of boreal NBP (Fig. S5a and c). In the northern temperate regions, all models (except CLM4CN) show negative γ_{NBP}^{int} with average of -0.44 ± 0.45 Pg C yr⁻¹ °C⁻¹ (Fig. S6b).

Response of NBP to precipitation variations (δ_{NBP}^{int})

The RLS is not significantly correlated with the precipitation (after statistically removing the contributive effect of temperature using partial correlation) at the global scale, but in contrast, eight of ten models still have a significant positive correlation between NBP and precipitation (all variables detrended) (Fig. 3b). Furthermore, nine models (except LPJ-GUESS) estimate a higher δ_{NBP}^{int} (average of 2.3 ± 1.6 Pg C yr⁻¹ per 100 mm of interannual precipitation change) compared with the observed RLS (0.8 ± 1.1 Pg C yr⁻¹ per 100 mm of interannual precipitation change) (Fig. 3b). These results indicate that current state-of-the-art carbon cycle models are likely to be too sensitive to precipitation variability. TRIFFID has the highest δ_{NBP}^{int} sensitivity (6.0 ± 0.9 Pg C yr⁻¹ per 100 mm) due to highest δ_{GPP}^{int} . Across 10 models, there is a significant positive correlation between global δ_{NBP}^{int} and δ_{GPP}^{int} with the slope of 0.61 ($R = 0.81$, $P < 0.01$). In addition, the model estimated response of fire emission to precipitation is much smaller than the intermodel differences in δ_{NBP}^{int} (Fig. S8).

It has been suggested that decreased CO₂ sinks in the next century over tropical regions, in response to soil drying, was one of the principal mechanisms explaining the positive carbon cycle–climate feedback diagnosed from the C4MIP coupled models (Friedlingstein *et al.*, 2006; Sitch *et al.*, 2008). In the tropics, all models (nine of 10 models significant) consistently produce a positive interannual covariance between precipitation and NBP. TRIFFID has the highest tropical δ_{NBP}^{int} (1.5 ± 0.2 Pg C yr⁻¹ per 100 mm), while ORCHIDEE shows the smallest tropical δ_{NBP}^{int} (0.3 ± 0.3 Pg C yr⁻¹ per 100 mm). In the extratropical regions, however, several models predict a negative response of NBP to wetter years, but the NBP–precipitation relationship is generally not significant (HYLAND, CLM4CN, and SDGVM only exhibit a significant relationship in the boreal region, and TRIFFID, LPJ, OCN in the northern temperate regions as shown by Fig. S7). In both boreal

and temperate regions, the highest δ_{NBP}^{int} was also simulated by the TRIFFID model due to its highest δ_{GPP}^{int} (Fig. S7a and b).

Response of NBP to rising atmospheric CO₂ concentration (β_{NBP})

From the average of the 10 models, we estimated β_{NBP} using the simulation S1 to be 2.39 ± 1.52 Pg C yr⁻¹ per 100 ppm at the global scale. CLM4CN shows the smallest β_{NBP} of 0.54 ± 2.79 Pg C yr⁻¹ per 100 ppm, which is only 23% of β_{NBP} in CLM4C. This shows that modeling nutrient limitation decreases the NBP sensitivity to atmosphere CO₂ concentration (Sokolov *et al.*, 2008; Thornton *et al.*, 2009; Zaehle *et al.*, 2010). ORCHIDEE has the largest β_{NBP} of 5.86 ± 2.02 Pg C yr⁻¹ per 100 ppm (Fig. 5b), probably due to its highest β_{GPP} compared with other models (Fig. 5a). Indeed, there is a significant correlation between β_{NBP} and β_{GPP} across 10 models ($P < 0.05$), suggesting that models have different β_{NBP} partly because of the different CO₂ fertilization effect on the vegetation growth (Ciais *et al.*, 2005). Among the 10 models, CLM4CN simulates the lowest carbon sequestration efficiency under rising atmospheric CO₂ concentration (4%), defined as the ratio of β_{NBP} to β_{GPP} , whereas ORCHIDEE has the highest carbon sequestration efficiency under rising atmospheric CO₂ concentration (20%). The ratio of β_{NBP} to β_{GPP} for the ensemble model average is about $12 \pm 4\%$.

Similar to β_{GPP} (Fig. 5a), β_{NBP} derived from simulation S2 and Eqn (3) is generally larger than β_{NBP} from simulation S1 (Fig. 5b), particularly in tropical regions (Fig. S10c). As shown in Fig. 5b, CLM4CN, OCN, SDGVM, and VEGAS estimated global β_{NBP} from the simulation S2 with Eqn (3) are smaller than the diagnosed sensitivity of RLS to atmospheric CO₂ (β_{RLS} , 8.12 ± 2.38 Pg C yr⁻¹ per 100 ppm) based on Eqn (3). However, it should be noted that since other factors such as ecosystem management and nitrogen deposition could also explain the trend of RLS over the last three decades (Zaehle *et al.*, 2006; Magnani *et al.*, 2007; Ciais *et al.*, 2008; Bellassen *et al.*, 2010; Zaehle & Dalmonech, 2011), the sensitivity of RLS to CO₂ from the Eqn (3) may be overestimated.

From model testing to directions for future research

To overcome the inevitable spread of curves resulting from a comparison of complex models with available observations, we investigated in this study the *contributive response* of models to climate variability, and compared the modeled response to the response diagnosed from available 'observations' (in fact other data-driven

models). The main contributive responses to interannual climate drivers are γ – the response to temperature anomalies in units of Pg C yr⁻¹ °C⁻¹, δ – the response to rainfall anomalies in units of Pg C yr⁻¹ 100 mm⁻¹, and β – the response to CO₂ trend, in units of Pg C yr⁻¹ 100 ppm⁻¹. Four key datasets are used to estimate these contributive responses, a data-oriented gridded GPP field (JU11), imposed warming experiments, imposed raised atmospheric CO₂ experiments (FACE) and the global residual land sink modeled to close the anthropogenic CO₂ budget (RLS). These four datasets provide information on different contributive responses, JU11 constrains γ , δ , and β of GPP, experimental warming site data constrain γ of NPP, the (scarce) FACE site data constrain β of NPP, and the RLS over 30 years constrains γ , δ , and β of NBP. We report the following new findings.

- 1 The 10 carbon cycle models give a higher mean GPP and a higher year-to-year GPP variability than the data-driven model of JU11, particularly in tropical regions. In tropical regions, the GPP interannual variance in JU11 can be considered too uncertain to be useable to falsify the process models. JU11 trained their MTE using *spatial gradients* among different sites (there are few long series) and extrapolated *temporal gradients*, confounding spatial and interannual sensitivity of GPP to climate. To overcome this limitations of comparing the uncertain process models with another uncertain data-driven model, we recommend future work to model at the site scale in which the measurements are made (in particular the long-term FLUXNET sites) to investigate their response to climate drivers for different time scales, and different ecosystems (Schwalm *et al.*, 2010). This will also require better protocols with site history to account for site specific disequilibrium of biomass and soil carbon pools (Carvalho *et al.* 2008).
- 2 The process models generally capture the interannual variation in the observed residual land carbon sink (RLS) estimation over the last three decades. But the models' contributive response to precipitation is too high, particularly in tropical forests and savannas (W. Wang, P. Ciais, R. Nemani, J. Canadell, S. Piao, S. Sitch, M. White, H. Hashimoto, C. Milesi, R. Myneni, submitted). It is not clear, however, if this too high contributive response of NBP to rainfall is induced by a bias of GPP or ecosystem respiration to soil moisture, or to an inaccurate representation of soil moisture by models. We recommend future work to compare the contributive response of net and gross CO₂ fluxes between models with independent large-scale flux estimations, such as from data-driven up-scaling of fluxes and top down inversions.

3 In response to interannual variation in temperature, all the models are found to simulate a stronger negative response of NBP than GPP, implying that respiration responds positively to temperature. To investigate this effect, we evaluated for the first time the global process models against site data from a collection of ecosystem warming experiments. We find that models tend to underpredict the response of NPP to temperature change at the temperate sites. However, it is difficult to tell from the warming experiments for NPP, which have significant between-site variation, whether this results predominantly from plant or soil respiration, or possibly both, where the balance varies strongly depending on geographical variation. The different approaches to derive the NPP response to temperature between global models forced offline by gridded climate data, and local field warming experiments that are coupled to the atmosphere, bias as well as the fact that process models do not consider subgrid scale heterogeneity in environmental conditions and vegetation distribution. We recommend to design a global benchmarking of carbon cycle models against ecosystem warming and drought experiments, and to compile a database of experiments results and forcing data that would be open access.

4 Despite the fact that carbon cycle models are often suspected to overestimate CO₂ fertilization as a driver of net land uptake, we found that the ensemble mean global NPP enhancement is comparable with FACE experiments observation. The CLM4CN model that have nitrogen limitations do show a sensitivity of NPP to CO₂ that is 50% lower than the same models versions (CLM4C) but without nitrogen. The strength of the CO₂ fertilization on the NBP is poorly quantified. The magnitude of NBP response to CO₂ is not merely dependent on the NPP response. NPP increases could create higher litterfall enhancing soil carbon stores also available to respire. We recommend all carbon cycle models should include nutrients, and pursue the evaluation of C–N interactions using both global and local observations (e.g., Zaehle *et al.*, 2010).

Overall, reducing these uncertainties of climate sensitivities of carbon fluxes is essential to more accurately predict future dynamics of the global carbon cycle and its feedbacks to climate system. This remains as a high priority for the carbon cycle modeling community. We recommend carbon cycle models to be run both ‘free running’ with their default parameters values used in global simulations, and ‘adjusted’ with parameters calibrated or optimized against site observations (e.g., warming, precipitation, and elevated CO₂ experiments, fluxnet data) so that the ‘portability’ of improvements

gained from small scale can be assessed at larger, regional, or global scale.

Acknowledgements

This study is part of the Regional Carbon Cycle Assessment and Processes (RECCAP), Global Carbon Project. We thank Dr. Law and three anonymous referees for the detailed and constructive comments. This work was supported by the National Natural Science Foundation of China (grant 41125004), National Basic Research Program of China (Grant No. 2010CB950601 and 2013CB956303), Foundation for Sino-EU research cooperation of Ministry of Science and Technology of China (1003), and CARBONES EU FP7 Foundation (242316). JGC is supported by the Australian Climate Change Science Program.

References

- Angert A, Biraud S, Bonfils C *et al.* (2005) Drier summers cancel out the CO₂ uptake enhancement induced by warmer springs. *Proceedings of the National Academy of Sciences of the United States of America*, **102**, 10823–10827.
- Arneeth A, Harrison SP, Zaehle S *et al.* (2010) Terrestrial biogeochemical feedbacks in the climate system. *Nature Geosciences*, **3**, 525–532.
- Bauerle WL, Oren R, Way DA *et al.* (2012) Photoperiodic regulation of the seasonal pattern of photosynthetic capacity and the implications for carbon cycling. *Proceedings of the National Academy of Sciences of the United States of America*, **109**, 8612–8617.
- Beck PS, Juday GP, Alix C *et al.* (2011) Changes in forest productivity across Alaska consistent with biome shift. *Ecology Letters*, **14**, 373–379.
- Ber C, Reichstein M, Tomelleri E *et al.* (2010) Terrestrial gross carbon dioxide uptake: global distribution and covariation with climate. *Science*, **329**, 834–838.
- Bellassen V, Le Maire G, Dhote JF, Ciais P, Viomy N (2010) Modelling forest management within a global vegetation model Part I: model structure and general behaviour. *Ecological Modelling*, **221**, 2458–2474.
- Blyth E, Clark DB, Ellis R *et al.* (2011) A comprehensive set of benchmark tests for a land surface model of simultaneous fluxes of water and carbon at both the global and seasonal scale. *Geoscientific Model Development*, **4**, 255–269.
- Boden, TA, Marland G, Andres RJ (2012) *Global, Regional, and National Fossil-Fuel CO₂ Emissions*. Carbon Dioxide Information Analysis Center, Oak Ridge National Laboratory, U.S. Department of Energy, Oak Ridge, TN, USA. doi: 10.3334/CDIAC/00001_V2012
- Bonan GB, Levis S (2010) Quantifying carbon-nitrogen feedbacks in the Community Land Model (CLM4). *Geophysical Research Letters*, **37**, L07401. doi: 10.1029/2010gl042430
- Cadule P, Friedlingstein P, Bopp L *et al.* (2010) Benchmarking coupled climate-carbon models against long-term atmospheric CO₂ measurements. *Global Biogeochemical Cycles*, **24**, GB2016. doi: 10.1029/2009gb003556
- Carvalhais N, Reichstein M, Seixas J *et al.* (2008) Implications of the carbon cycle steady state assumption for biogeochemical modeling performance and inverse parameter retrieval. *Global Biogeochemical Cycles*, **22**, GB2007. doi: 10.1029/2007GB003033
- Ciais P, Tans PP, Trolier M, White JWC, Francey RJ (1995) A Large Northern Hemisphere Terrestrial CO₂ Sink Indicated by the 13C/12C Ratio of Atmospheric CO₂. *Science*, **269**, 1098–1102.
- Ciais P, Reichstein M, Viomy N *et al.* (2005) Europe-wide reduction in primary productivity caused by the heat and drought in 2003. *Nature*, **437**, 529–533.
- Ciais P, Schelhaas MJ, Zaehle S *et al.* (2008) Carbon accumulation in European forests. *Nature Geoscience*, **1**, 425–429.
- Clark DA, Piper SC, Keeling CD, Clark DB (2003) Tropical rain forest tree growth and atmospheric carbon dynamics linked to interannual temperature variation during 1984–2000. *Proceedings of the National Academy of Sciences*, **100**, 5852–5857.
- Clark DB, Olivas PC, Oberbauer SF, Clark DA, Ryan MG (2008) First direct landscape-scale measurement of tropical rain forest Leaf Area Index, a key driver of global primary productivity. *Ecology Letters*, **11**, 163–172.
- Conway TJ, Tans PP, Waterman LS, Thoning KW, Kitzis DR, Masarie KA, Zhang N (1994) Evidence for interannual variability of the carbon cycle from the National Oceanic and Atmospheric Administration/Climate Monitoring and Diagnostics Laboratory Global Air Sampling Network. *Journal Of Geophysical Research*, **99**, 22831–22855.

- Corlett RT (2011) Impacts of warming on tropical lowland rainforests. *Trends in Ecology & Evolution*, **26**, 606–613.
- Cox PM (2001) Description of the TRIFFID dynamic global vegetation model. Technical Note 24 Hadley Centre, Met Office.
- Cox P, Jones C (2008) Illuminating the modern dance of climate and CO₂. *Science*, **321**, 1642–1644.
- Cox PM, Betts RA, Jones CD, Spall SA, Totterdell IJ (2000) Acceleration of global warming due to carbon-cycle feedbacks in a coupled climate model. *Nature*, **408**, 184–187.
- Cramer W, Bondeau A, Woodward FI *et al.* (2001) Global response of terrestrial ecosystem structure and function to CO₂ and climate change: results from six dynamic global vegetation models. *Global Change Biology*, **7**, 357–373.
- Da Costa ACL, Galbraith D, Almeida S *et al.* (2010) Effect of 7 yr of experimental drought on vegetation dynamics and biomass storage of an eastern Amazonian rainforest. *New Phytologist*, **187**, 579–591.
- Doughty CE, Goulden ML (2008) Are tropical forests near a high temperature threshold? *Journal of Geophysical Research: Biogeosciences*, **113**, G00B07. doi: 10.1029/2007JG000632
- Denman K, Brasseur G, Chidthaisong A *et al.* (2007) "Couplings Between Changes in the Climate System and Biogeochemistry" in *Climate Change 2007: The Physical Science Basis, Contribution of Working Group I to the Fourth Assessment Report of the Intergovernmental Panel on Climate Change*. Cambridge University Press, Cambridge, United Kingdom and United States.
- Frank DC, Esper J, Raible CC, Buntgen U, Trouet V, Stocker B, Joos F (2010) Ensemble reconstruction constraints on the global carbon cycle sensitivity to climate. *Nature*, **463**, 527–530.
- Friedlingstein P, Cox P, Betts R *et al.* (2006) Climate-carbon cycle feedback analysis: results from the (CMIP)-M-4 model intercomparison. *Journal of Climate*, **19**, 3337–3353.
- Friedlingstein P, Houghton RA, Marland G *et al.* (2010) Update on CO₂ emissions. *Nature Geoscience*, **3**, 811–812.
- Hickler T, Smith B, Prentice IC, Mjöfors K, Miller P, Arneith A, Sykes MT (2008) CO₂ fertilization in temperate FACE experiments not representative of boreal and tropical forests. *Global Change Biology*, **14**, 1531–1542.
- Houghton RA (1999) The annual net flux of carbon to the atmosphere from changes in land use 1850–1990. *Tellus Series B-chemical And Physical Meteorology*, **51**, 298–313.
- Houghton RA (2007) Balancing the global carbon budget. *Annual Review Of Earth And Planetary Sciences*, **35**, 313–347.
- Houghton RA (2010) How well do we know the flux of CO₂ from land-use change? *Tellus Series B-Chemical And Physical Meteorology*, **62**, 337–351.
- Hungate BA, Dukes JS, Shaw MR, Luo YQ, Field CB (2003) Nitrogen and climate change. *Science*, **302**, 1512–1513.
- Huntingford C, Lowe JA, Booth BBB, Jones CD, Harris GR, Gohar LK, Meir P (2009) Contributions of carbon cycle uncertainty to future climate projection spread. *Tellus Series B-Chemical And Physical Meteorology*, **61**, 355–360.
- Huntingford C, Cox PM, Mercado LM, Sitch S, Bellouin N, Boucher O, Gedney N (2011) Highly contrasting effects of different climate forcing agents on terrestrial ecosystem services. *Philosophical Transactions of the Royal Society A-Mathematical, Physical and Engineering Sciences*, **369**, 2026–2037.
- IPCC (2007) *The Physical Science Basis: Summary for Policymakers*. Intergovernmental Panel on Climate Change Secretariat, Geneva.
- Iversen CM, Ledford J, Norby RJ (2008) CO₂ enrichment increases carbon and nitrogen input from fine roots in a deciduous forest. *New Phytologist*, **179**, 837–847.
- Jung M, Le Maire G, Zaehle S *et al.* (2007) Assessing the ability of three land ecosystem models to simulate gross carbon uptake of forests from boreal to Mediterranean climate in Europe. *Biogeosciences*, **4**, 647–656.
- Jung M, Reichstein M, Margolis HA *et al.* (2011) Global patterns of land-atmosphere fluxes of carbon dioxide, latent heat, and sensible heat derived from eddy covariance, satellite, and meteorological observations. *Journal Of Geophysical Research*, **116**, G00J07. doi: 10.1029/2010jg001566
- Keeling CD, Whorf TP (2005) Atmospheric CO₂ records from sites in the SIO sampling network. In: *Trends: A Compendium of Data on Global Change*. Carbon Dioxide Information Analysis Center, Oak Ridge National Laboratory, US Department of Energy, Oak Ridge, TN, USA. <http://cdiac.ornl.gov/trends/co2/sio-mlo.htm>
- Keenan TF, Davidson E, Moffat AM, Munger W, Richardson AD (2012) Using model-data fusion to interpret past trends, and quantify uncertainties in future projections, of terrestrial ecosystem carbon cycling. *Global Change Biology*, **18**, 2555–2569.
- Krinner G, Viovy N, De Noblet-Ducoudré N *et al.* (2005) A dynamic global vegetation model for studies of the coupled atmosphere-biosphere system. *Global Biogeochemical Cycles*, **19**, GB1015. doi: 10.1029/2003gb002199
- Lasslop G, Reichstein M, Papale D *et al.* (2010) Separation of net ecosystem exchange into assimilation and respiration using a light response curve approach: critical issues and global evaluation. *Global Change Biology*, **16**, 187–208.
- Lawrence D, Oleson KW, Flanner MG *et al.* (2011) Parameterization improvements and functional and structural advances in version 4 of the community land model. *Journal of Advances in Modeling Earth Systems*, **3**. doi: 10.1029/2011ms000045
- Le Quere C, Raupach MR, Canadell JG *et al.* (2009) Trends in the sources and sinks of carbon dioxide. *Nature Geoscience*, **2**, 831–836.
- Levy PE, Cannell MGR, Friend AD (2004) Modelling the impact of future changes in climate, CO₂ concentration and land use on natural ecosystems and the terrestrial carbon sink. *Global Environmental Change*, **14**, 21–30.
- Long SP, Ainsworth EA, Leakey ADB, Nösberger J, Ort DR (2006) Food for thought: lower-than-expected crop yield stimulation with rising CO₂ concentrations. *Science*, **312**, 1918–1921.
- Lu M, Zhou X, Luo Y *et al.* (2013) Responses of ecosystem carbon cycle to experimental warming: a meta-analysis. *Ecology*. doi: 10.1890/12-0279.1
- Lucht W, Prentice IC, Myneni RB *et al.* (2002) Climatic control of the high-latitude vegetation greening trend and Pinatubo effect. *Science*, **296**, 1687–1689.
- Luo Y (2007) Terrestrial carbon-cycle feedback to climate warming. *Annual Review of Ecology, Evolution, and Systematics*, **38**, 683–712.
- Magnani F, Mencuccini M, Borghetti M *et al.* (2007) The human footprint in the carbon cycle of temperate and boreal forests. *Nature*, **447**, 848–850.
- Matthews HD (2005) Decrease of emissions required to stabilize atmospheric CO₂ due to positive carbon cycle-climate feedbacks. *Geophysical Research Letters*, **32**, L21707. doi: 10.1029/2005GL023435
- Mcgrath GS, Sadler R, Fleming K, Gregoning P, Hinz C, Veneklaas EJ (2012) Tropical cyclones and the ecohydrology of Australia's recent continental-scale drought. *Geophysical Research Letters*, **39**, L03404. doi: 10.1029/2011gl050263
- Melillo JM, Steudler PA, Aber JD *et al.* (2002) Soil warming and carbon-cycle feedbacks to the climate system. *Science*, **298**, 2173–2176.
- Moorcroft PR (2006) How close are we to a predictive science of the biosphere? *Trends in Ecology & Evolution*, **21**, 400–407.
- Myneni RB, Keeling CD, Tucker CJ, Asrar G, Nemani RR (1997) Increased plant growth in the northern high latitudes from 1981 to 1991. *Nature*, **386**, 698–702.
- Nepstad DC, Moutinho P, Dias-Filho MB *et al.* (2002) The effects of partial throughfall exclusion on canopy processes, aboveground production, and biogeochemistry of an Amazon forest. *Journal Of Geophysical Research*, **107**, 8085. doi: 10.1029/2001jd000360
- Nepstad D, Lefebvre P, Lopes Da Silva U *et al.* (2004) Amazon drought and its implications for forest flammability and tree growth: a basin-wide analysis. *Global Change Biology*, **10**, 704–717.
- Norby RJ, Delucia EH, Gielen B *et al.* (2005) Forest response to elevated CO₂ is conserved across a broad range of productivity. *Proceedings of the National Academy of Sciences of the United States of America*, **102**, 18052–18056.
- Oleson KW, Lawrence DM, Gordon B *et al.* (2010) *Technical description of version 4.0 of the Community Land Model (CLM)*. NCAR/TN-478+STR. NCAR, Boulder, USA.
- Pan Y, Birdsey RA, Fang J *et al.* (2011) A Large and Persistent Carbon Sink in the World's Forests. *Science*, **333**, 988–993.
- Phillips OL, Aragão LEOC, Lewis SL *et al.* (2009) Drought Sensitivity of the Amazon Rainforest. *Science*, **323**, 1344–1347.
- Phillips OL, Van Der Heijden G, Lewis SL *et al.* (2010) Drought-mortality relationships for tropical forests. *New Phytologist*, **187**, 631–646.
- Piao S, Friedlingstein P, Ciais P, Zhou L, Chen A (2006) Effect of climate and CO₂ changes on the greening of the Northern Hemisphere over the past two decades. *Geophysical Research Letters*, **33**, L23402. doi: 10.1029/2006gl028205
- Piao SL, Friedlingstein P, Ciais P, Viovy N, Demarty J (2007) Growing season extension and its impact on terrestrial carbon cycle in the Northern Hemisphere over the past 2 decades. *Global Biogeochemical Cycles*, **21**, 49–53. doi: 10.1029/2006gb002888
- Piao SL, Ciais P, Friedlingstein P *et al.* (2008) Net carbon dioxide losses of northern ecosystems in response to autumn warming. *Nature*, **451**, 49–53.
- Piao S, Ciais P, Friedlingstein P, De Noblet-Ducoudré N, Cadule P, Viovy N, Wang T (2009a) Spatiotemporal patterns of terrestrial carbon cycle during the 20th century. *Global Biogeochemical Cycles*, **23**, GB4026. doi: 10.1029/2008gb003339
- Piao S, Friedlingstein P, Ciais P, Peylin P, Zhu B, Reichstein M (2009b) Footprint of temperature changes in the temperate and boreal forest carbon balance. *Geophysical Research Letters*, **36**, L07404. doi: 10.1029/2009gl037381
- Poulter B, Aragão L, Heyder U *et al.* (2010) Net biome production of the Amazon Basin in the 21st century. *Global Change Biology*, **16**, 2062–2075.
- Poulter B, Frank DC, Hodson EL, Zimmermann NE (2011) Impacts of land cover and climate data selection on understanding terrestrial carbon dynamics and the CO₂ airborne fraction. *Biogeosciences*, **8**, 2027–2036.

- Randerson JT, Hoffman FM, Thornton PE *et al.* (2009) Systematic assessment of terrestrial biogeochemistry in coupled climate-carbon models. *Global Change Biology*, **15**, 2462–2484.
- Richardson AD, Andy Black T, Ciais P *et al.* (2010) Influence of spring and autumn phenological transitions on forest ecosystem productivity. *Philosophical Transactions of the Royal Society B-Biological Sciences*, **365**, 3227–3246.
- Scheffer M, Brovkin V, Cox PM (2006) Positive feedback between global warming and atmospheric CO₂ concentration inferred from past climate change. *Geophysical Research Letters*, **33**, L10702. doi: 10.1029/2005gl025044
- Schimel DS, House JJ, Hibbard KA *et al.* (2001) Recent patterns and mechanisms of carbon exchange by terrestrial ecosystems. *Nature*, **414**, 169–172.
- Schwalm CR, Williams CA, Schaefer K *et al.* (2010) A model-data intercomparison of CO₂ exchange across North America: results from the North American Carbon Program site synthesis. *Journal of Geophysical Research*, **115**, G00H05. doi: 10.1029/2009JG001229
- Sitch S, Smith B, Prentice IC *et al.* (2003) Evaluation of ecosystem dynamics, plant geography and terrestrial carbon cycling in the LPJ dynamic global vegetation model. *Global Change Biology*, **9**, 161–185.
- Sitch S, Huntingford C, Gedney N *et al.* (2008) Evaluation of the terrestrial carbon cycle, future plant geography and climate-carbon cycle feedbacks using five Dynamic Global Vegetation Models (DGVMs). *Global Change Biology*, **14**, 2015–2039.
- Smith B, Prentice IC, Sykes MT (2001) Representation of vegetation dynamics in the modelling of terrestrial ecosystems: comparing two contrasting approaches within European climate space. *Global Ecology And Biogeography*, **10**, 621–637.
- Sokolov AP, Kicklighter DW, Melillo JM, Felzer BS, Schlosser CA, Cronin TW (2008) Consequences of considering carbon-nitrogen interactions on the feedbacks between climate and the terrestrial carbon cycle. *Journal Of Climate*, **21**, 3776–3796.
- Stephens BB, Gurney KR, Tans PP *et al.* (2007) Weak northern and strong tropical land carbon uptake from vertical profiles of atmospheric CO₂. *Science*, **316**, 1732–1735.
- Stöckli R, Lawrence DM, Niu GY *et al.* (2008) Use of FLUXNET in the Community Land Model development. *Journal Of Geophysical Research*, **113**, G01025. doi: 10.1029/2007jg000562
- Thornton PE, Doney SC, Lindsay K *et al.* (2009) Carbon-nitrogen interactions regulate climate-carbon cycle feedbacks: results from an atmosphere-ocean general circulation model. *Biogeosciences*, **6**, 2099–2120.
- Tribuzy ES (2005) Variacoes da temperatura foliar do dossel e o seu efeito na taxa assimilatoria de CO₂ na Amazonia Central. Ph.D. dissertation. Univ. de Sao Paulo, Sao Paulo.
- Van Oss HG (2008) *2006 Minerals Yearbook 16.1–16.36*. US Geological Survey.
- Wang W, Wang W-J, Li J-S, Wu H, Xu C, Liu T (2010) The Impact of Sustained Drought on Vegetation Ecosystem in Southwest China Based on Remote Sensing. *Procedia Environmental Sciences*, **2**, 1679–1691.
- Wang X, Piao S, Ciais P, Li J, Friedlingstein P, Koven C, Chen A (2011) Spring temperature change and its implication in the change of vegetation growth in North America from 1982 to 2006. *Proceedings of the National Academy of Sciences*, **108**, 1240–1245.
- Welp LR, Keeling RF, Haj Meijer *et al.* (2011) Interannual variability in the oxygen isotopes of atmospheric CO₂ driven by El Nino. *Nature*, **477**, 579–582.
- Woodward FI, Lomas MR (2004) Simulating vegetation processes along the Kalahari transect. *Global Change Biology*, **10**, 383–392.
- Woodward FI, Smith TM, Emanuel WR (1995) A global land primary productivity and phytogeography model. *Global Biogeochemical Cycles*, **9**, 471–490.
- Van Oss HG (2008) *2006 Minerals Yearbook 16.1–16.36*. US Geological Survey.
- Zaehle S, Dalmonech D (2011) Carbon-nitrogen interactions on land at global scales: current understanding in modelling climate biosphere feedbacks. *Current Opinion in Environmental Sustainability*, **3**, 311–320.
- Zaehle S, Friend AD, Friedlingstein P, Dentener F, Peylin P, Schulz M (2010) Carbon and nitrogen cycle dynamics in the O-CN land surface model: 2. Role of the nitrogen cycle in the historical terrestrial carbon balance. *Global Biogeochemical Cycles*, **24**, GB1006. doi: 10.1029/2009GB003522
- Zaehle S, Friend AD (2010) Carbon and nitrogen cycle dynamics in the O-CN land surface model: 1. Model description, site-scale evaluation, and sensitivity to parameter estimates. *Global Biogeochemical Cycles*, **24**, GB1005. doi: 10.1029/2009gb003521
- Zaehle S, Sitch S, Prentice IC *et al.* (2006) The importance of age-related decline in forest npp for modeling regional carbon balances. *Ecological Applications*, **16**, 1555–1574.
- Zeng N, Mariotti A, Wetzel P (2005a) Terrestrial mechanisms of interannual CO₂ variability. *Global Biogeochemical Cycles*, **19**, GB1016. doi: 10.1029/2004gb002273
- Zeng N, Qian H, Roedenbeck C, Heimann M (2005b) Impact of 1998–2002 midlatitude drought and warming on terrestrial ecosystem and the global carbon cycle. *Geophysical Research Letters*, **32**, L22709. doi: 10.1029/2005gl024607
- Zhang X, Goldberg M, Tarpley D, Friedl MA, Morissette J, Kogan F, Yu Y (2010) Drought-induced vegetation stress in southwestern North America. *Environmental Research Letters*, **5**, 024008.
- Zhao M, Running SW (2010) Drought-induced reduction in global terrestrial net primary production from 2000 through 2009. *Science*, **329**, 940–943.

Supporting Information

Additional Supporting Information may be found in the online version of this article:

Figure S1. Comparison of carbon flux (Gross Primary Production (GPP) and Net Biome Productivity (NBP)) response to interannual variations in climate estimated by two approaches.

Figure S2. The magnitude of regional Gross Primary Production (GPP) during 1982–2008 estimated by the 10 carbon cycle models and a data driven model tree ensemble approach (JU11, Jung *et al.*, 2011) and Net Biome Productivity (NBP) during 1980–2009 estimated by the 10 carbon cycle models during 1980–2009 over four different regions.

Figure S3. Cumulative frequency distribution for Gross Primary Production (GPP) during 1982–2008.

Figure S4. Correlation matrix displaying correlation coefficient between pairs of detrended anomalies of regional Gross Primary Production (GPP) during 1982–2008.

Figure S5. Correlation matrix displaying correlation coefficient between pairs of detrended anomalies of regional Net Biome Productivity (NBP) during 1980–2009.

Figure S6. The response of regional Gross Primary Production (GPP) and regional Net Biome Production (NBP) to interannual variation in temperature and interannual variation in precipitation during 1982–2008 over four different regions.

Figure S7. The response of regional Gross Primary Production (GPP) and regional Net Biome Production (NBP) to interannual variation in precipitation and interannual variation in precipitation during 1982–2008 over four different regions.

Figure S8. Comparison of (a) the response of global Net Biome Productivity (NBP) to interannual variations in temperature and the response of the sum in NBP and fire emission to interannual variations in temperature, (b) the response of global NBP to interannual variations in precipitation and the response of the sum in NBP and fire emission to interannual variations in precipitation.

Figure S9. The response of regional Gross Primary Production (GPP) to rising atmospheric CO₂ concentration during 1982–2008 over four different regions.

Figure S10. The response of regional Net Biome Productivity (NBP) to rising atmospheric CO₂ concentration during 1980–2009 over different regions.

Table S1. Ten carbon cycle models used in this study.

Table S2. Characteristics of warming experiment sites in this study.

Table S3. Site characteristics of FACE experiment sites in this study.